Flomeko 2000 - IMEKO TC9 Conference
Salvador, Bahia, BRAZIL
4-8 June, 2000

EXPERIMENTAL INVESTIGATION ON CRITICAL FLOW THROUGH MICROORIFICES AND CAPILLARIES

Kazuto Kawakita and Marcos Tadeu Pereira

IPT-Institute for Technological Research
Cidade Universitária, São Paulo-SP, BRAZIL

Abstract. *With the purpose of studying application of critical flows through small orifices in the measurement and control of very low gas flowrates, experimental investigations were carried out on a set of 22 microorifices and capillaries of circular cross sections manufactured out of ruby and stainless steel. Diameters of the orifice and capillary samples ranged from 16㎜ to 427㎜, and their lengths from 254㎜ to 68mm. The microorifices were submitted to tests using air, argon, helium and carbon dioxide, and the back to the upstream pressure ratio P_b/P_0 varied from unity down to about 0,1, both under pressure and vacuum operations. Results showed that, when operating under vacuum, the critical flow regime indicates that the discharge coefficient is stable and choking occurs even in flows with very small Reynolds numbers. However, when operating under pressure, the critical flow regime depends on the pressure ratio P_b/P_0, and other parameters related to the gas properties and the orifice dimensions. Experimental results also showed that compressibility factor is a fundamental parameter to be considered in critical flows through microorifices, mainly when operating under a pressurized condition.*

Keywords: microorifices, capillaries, critical flow, compressible flow, and microflows.

1. INTRODUCTION

The nature of fluid flow in relatively large macroscale structures such as pipes, tanks and even at open conditions has been a matter for experimental and theoretical investigations since antiquity. In this way, the enormous amount of studies carried out mostly during the second part of the 20th century has contributed to the development of the classical fluid mechanics. Under the point of view of fluid flow metrology, this knowledge has set the basis and the principles of operation of many fluid flowmeters.

Conversely, microescale fluid flows have not attracted much attention due both to experimental limitations and a perceived lack of importance of these flows. Microescale flows are no less common or less significant than flows that occur on a larger scale, they are just harder to perceive and observe. In fact, precise measurement of small flowrates are present demands on industrial and scientific activities, especially in applications related to gas flowrate control in chemical processes, bioengineering, microelectromechanical systems, and many other fields. Application demands also come from well-established industries, as a result of the increasing trends for automation and miniaturization, including requirements for fluid flow measurements at better levels.

In this scenery where scaling down flowmeter sizes becomes a manufacturing problem, critical flow elements reveals to be a suitable solution for the measurement and control of small gas flowrates. Although theory of operation of large critical nozzles is available in the literature and the ISO 9300 standard establishes the conditions for design and operation of cylindrical and toroidal throat sonic nozzles, critical flow elements of small sizes have not been a matter of investigations until recent years. Thus, as a result of an extensive experimental investigation, some of the characteristics of critical flow regimes through microorifices and capillaries will be shown in this paper.

2. MICRODEVICES USED IN THE INVESTIGATION

Miniaturization is indeed a limiting factor in the manufacturing process of small restriction elements, making it difficult the generation of convergent-divergent profiles characteristic of larger nozzles. Due to this fact, the present investigation was carried out using cylindrical microorifices made out of ruby and stainless steel capillaries of circular cross section, whose fabrication is comparatively easier than that of the nozzles.

Microorifices manufactured out of ruby. Synthetic ruby is exceptionally smooth on the surface as well as being extremely hard, presenting 9 on the Mohs scale where diamond, the hardest material, equals 10. It also offers great compressive strength and a high resistance to mechanical corrosion. Practically free from wear, ruby doesn`t adhere to metal through friction even at high temperatures.

The investigation was carried out using 14 different microorifices made out of ruby, all of them with a circular hole length of 254 μm and presenting internal diameters in the range of 16 a 423 μm. Bore were sharp-edged in the cross sectional plane of both ends. Figure 1 shows schematically the ruby made microorifice and table 1 presents the basic dimensions of the samples used in the investigation.

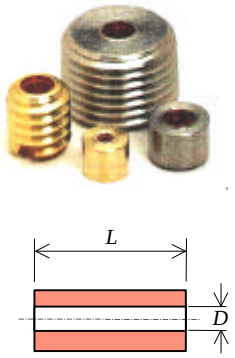

Figure 1. Ruby made microorifices.

Table 1. Basic dimensions of the ruby microorifices.

Bore length *L* [μm]	Diameter *D* [μm]	Relation *L*/*D*	Sample identification
254	423	0,60	*D*423*L*0.60
254	316	0,80	*D*316*L*0.80
254	265	0,96	*D*265*L*0.96
254	218	1,2	*D*218*L*1.20
254	170	1,5	*D*170*L*1.50
254	113	2,2	*D*113*L*2.20
254	100	2,5	*D*100*L*2.50
254	86	3,0	*D*086*L*3.00
254	76	3,3	*D*076*L*3.30
254	67	3,8	*D*067*L*3.80
254	48	5,3	*D*048*L*5.30
254	34	7,4	*D*034*L*7.40
254	24	11	*D*024*L*11.0
254	16	16	*D*016*L*16.0

Note: Samples are identified according to a code. For instance, *D*423*L*0.60, refers to the sample of diameter *D* equal to 423μm, and with a specific length *L* which establishes a *L*/*D* relation of 0,60.

Stainless steel capillaries. The investigation of friction (Fanno) flows at critical conditions in capillaries with large length to diameter ratios was carried out using a set of 8 small tubes of 427μm internal diameter. Samples were manufactured in different lengths, establishing *L*/*D* relations in the range of 8 to 160. Figure 2 shows the group of capillaries, and table 2 presents the basic dimensions of the samples used in the experimental investigation.

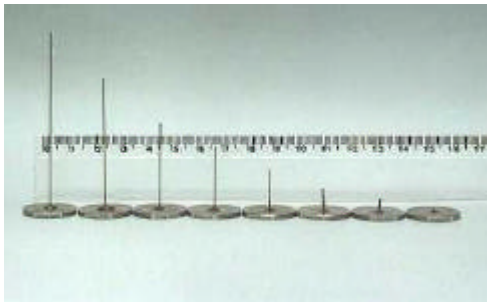

Figure 2. Set of capillary samples.

Table 2. Basic dimensions of the capillary samples.

Length *L* [mm]	Diameter *D* [μm]	Relation *L*/*D*	Sample identification
3,4	427	8	*D*427*L*008
6,8	427	16	*D*427*L*016
10,2	427	24	*D*427*L*024
17,0	427	40	*D*427*L*040
25,5	427	60	*D*427*L*060
34,0	427	80	*D*427*L*080
51,0	427	120	*D*427*L*120
68,0	427	160	*D*427*L*160

3. EXPERIMENTAL APPARATUS

Each sample under test was installed inside a special holder and between two chambers called upstream and downstream reservoirs. Dimensions of these reservoirs were comparatively larger than those of the devices tested, allowing flow conditions for the measurement of pressure and temperature.

Pressurized tests on critical flow regime through the orifices were established by increasing the stagnation pressure P_0 in the upstream reservoir, maintaining the back pressure P_b at constant level, and establishing different P_b/P_0 relations. On the other hand, tests under vacuum were conducted by gradually reducing the back pressure P_b and maintaining the stagnation pressure P_0 constant and close to the atmospheric pressure. Consequently, the experimental apparatus was conceived to permit tests to be carried out in both under pressure and under vacuum operations. Figure 3 shows the apparatus used in the experimental investigation.

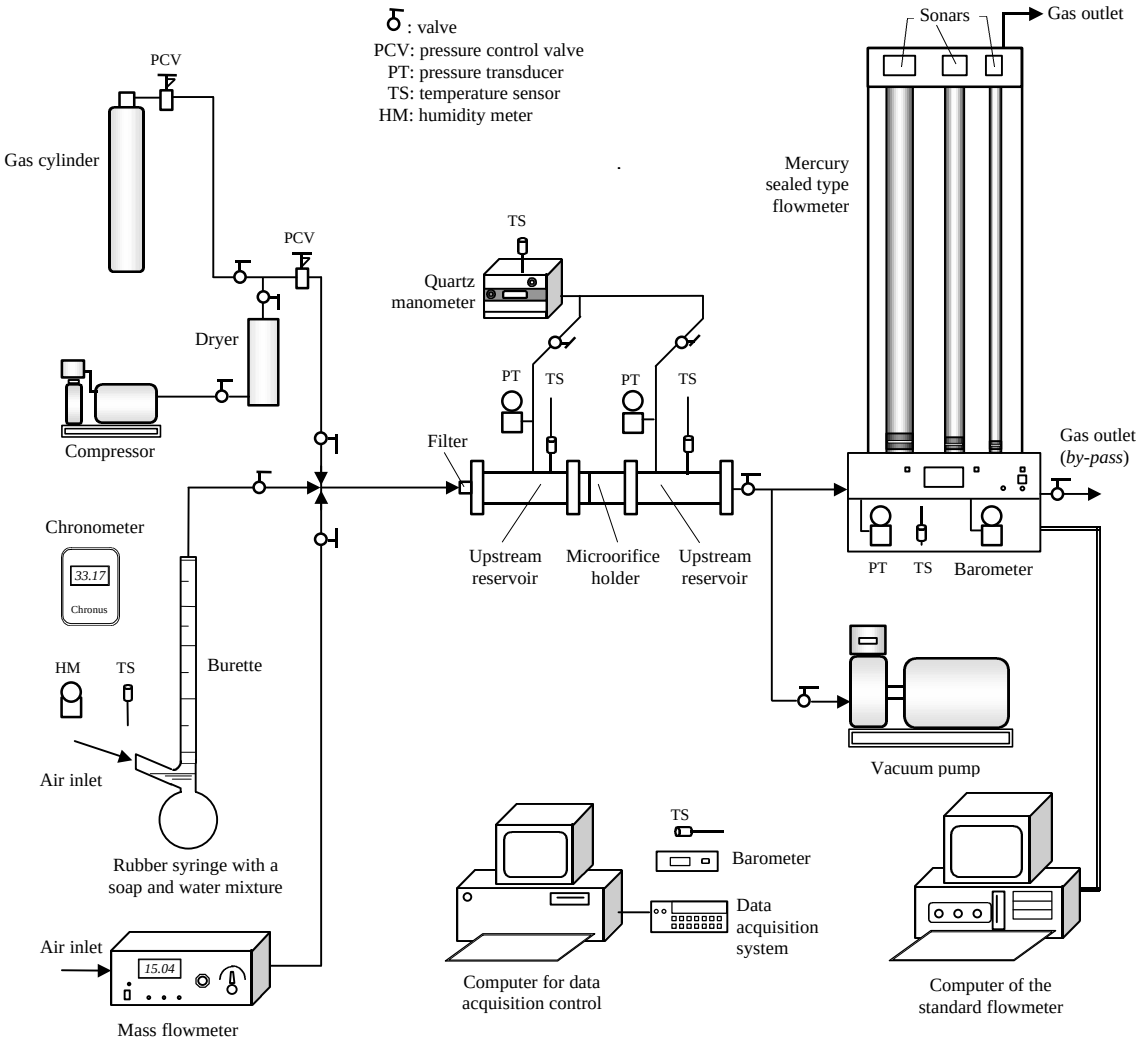

Figure 3. Experimental apparatus.

Flow properties determination

In the experimental investigation the basic parameters measured in the tests of each sample and at each particular operation condition were the gas mass flowrate ($\dot{m}$), the stagnation pressure and temperature (P_0, T_0) and the back pressure (P_b). Obviously, considering the physical limitations of the microorifices, parameters related to the flow conditions close or inside the restriction element were not possible to be measured.

4. RESULTS

4.1 Results obtained for the ruby samples

Ruby microorifices were submitted to tests under upstream pressurized conditions using dry air, argon, CO_2 and helium. Tests carried out by reducing back pressure were performed using ambient air.

Volumetric flowrate (Q_0) referred to the upstream stagnation conditions

Although experimental results make it possible the graphic representation of a series of parameters, normally, the stability of the volumetric flowrate of the gas, referred to the stagnation conditions (Q_0), is a useful parameter to indicate the critical flow conditions.

Figures 4 to 7 show the results of the volumetric flowrate Q_0 in terms of the pressure ratio P_b/P_0 for the ruby made samples operating under pressure with air, argon, CO_2 and helium. Figure 8 presents the results for an operation under vacuum using ambient air.

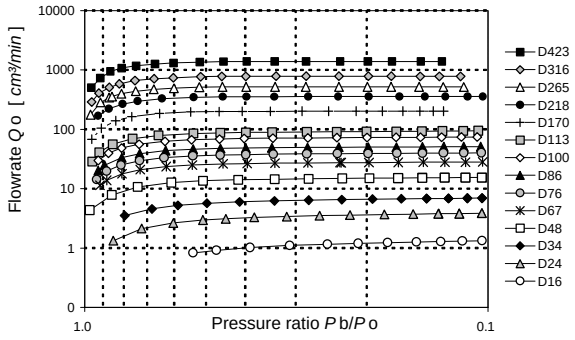

Figure 4. Flowrate Q_0 of air versus pressure ratio P_b/P_0 (ruby orifices, operation under pressure).

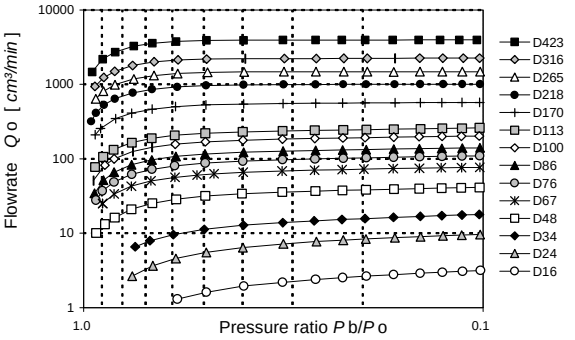

Figure 7. Flowrate Q_0 of helium versus pressure ratio P_b/P_0 (ruby orifices, operation under pressure).

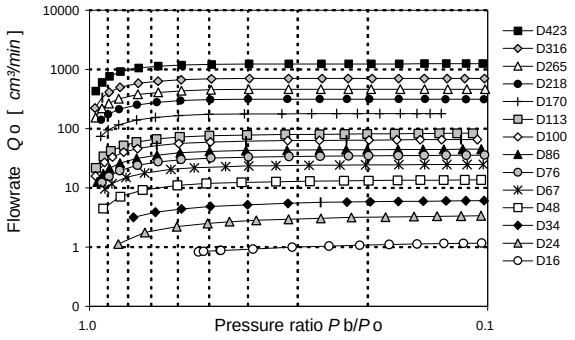

Figure 5. Flowrate Q_0 of argon versus pressure ratio P_b/P_0 (ruby orifices, operation under pressure).

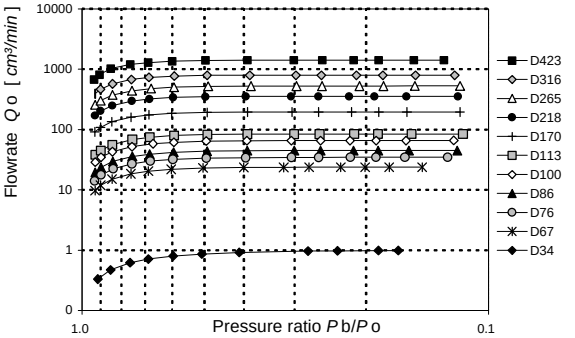

Figure 8. Flowrate Q_0 of air versus pressure ratio P_b/P_0 (ruby orifices, operation under vacuum).

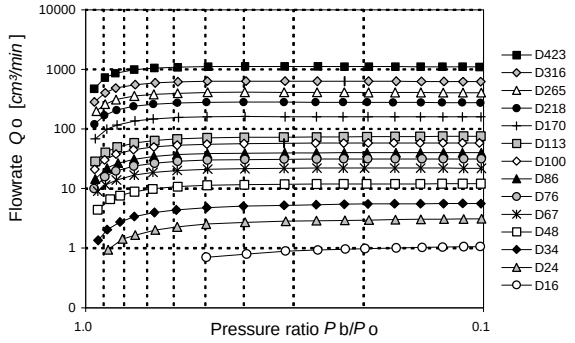

Figure 6. Flowrate Q_0 of CO_2 versus pressure ratio P_b/P_0 (ruby orifices, operation under pressure).

The shapes of curves in the bi-logarithm graphics indicate, for all the gases used, an evident tendency to increase the volumetric flowrate as the pressure ratio P_b/P_0 is reduced. However, this increase is much more evident for the case of an operation with helium than with the other gases. This different behaviour can be explained through the critical velocity V^*, i.e., the velocity of the gas when the Mach number is unity. For an adiabatic flowrate of a perfect gas, the critical velocity is given by:

$$V^* \equiv a^* = \sqrt{\frac{2k}{k+1} RT_0} \qquad (1)$$

where a^* is the velocity of the sound at Mach number unity, k is the gas specific heat ratio, R is the gas constant and T_0 is the absolute temperature of the gas. In order to provide a simple comparison, table 3 presents the values for the molar mass M, the gas constant R, the gas specific heat ratio k, and the velocity of sound at 20°C for the gases used in the investigation.

Table 3. Properties of the gases used in the investigation.

Gas	Molar mass of the gas M [kg/kmol]	Gas constant R [J/kg K]	Gas specific heat ratio $k=c_p/c_v$ at 20°C	Velocity of the sound at 20°C [m/s]	Critical velocity at 20°C [m/s]
Air	28,9645	287,055	1,4	43	313
Argon	39,948	208,131	1,66	318	276
CO_2	44,0098	188,921	1,288	267	250
Helium	4,0026	2077,252	1,659	1005	871

Data from: N.V. Nederlandse Gasunie, **Physical Properties of natural gases.** Groningen (1988).

Considering a stagnation temperature of 20°C (T_0=293,15K), table 3 shows that, according to equation (1), critical velocity for helium is much higher than for other gases and, consequently, the volumetric flowrate referred to the stagnation conditions Q_0 is comparatively much higher for helium than for other gases.

Choking under pressure and under vacuum

Based on the graphics presented in figures 4 to 7, referred to the pressurized operation condition, it is possible to observe that, by gradually increasing the stagnation pressure P_0, what means a reduction in the pressure ratio P_b/P_0, there is a tendency to stabilize the volumetric flowrate Q_0 showing the establishment of a critical flow regime. The same effect can be observed in the case of an operation under vacuum through the graphics in figure 8 where the back pressure P_b is gradually reduced.

However, it is interesting to note that the critical flow regime for an operation under pressure is not the same for an operation under vacuum, as can be seen in figure 9 bellow. In this figure, experimental results of volumetric flowrate Q_0 against the pressure ratio P_b/P_0 are plotted for the ruby made microorifice *D*423*L*0.60 (*D* diameter of 423µm and *L*/*D* relation of 0,60). These results are the same presented for each gas in figures 4 to 8, but for the sake of a better visualisation the flowrate, scale is maximised. In the case of helium, considering that the absolute values of the data are much higher than the one for other gases, the same are referred to the right hand vertical scale in figure 9.

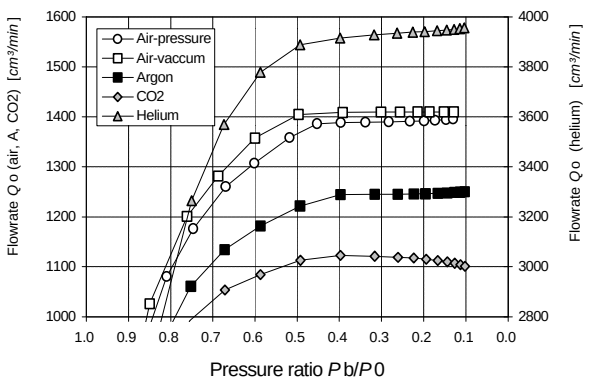

Figure 9. Volumetric flowrate Q_0 of the gases versus pressure ratio P_b/P_0 (ruby *D*423*L*0.60, operation under pressure and under vacuum).

Based on the results presented, it is possible to observe that, for air, the critical flow regime under vacuum operation provides a constant volumetric flowrate Q_0 versus the pressure ratio P_b/P_0.

Conversely, the critical flow regime under pressure do not maintain the volumetric flowrate Q_0 constant, i.e., it is possible to see a small variation in this parameter with a decrease in the pressure ratio P_b/P_0 even after the critical flow regime is established. This effect is also observed for the case of operation under pressurized regime with argon and helium that present a similar behaviour to that obtained for air.

To explain this increase in the volumetric flowrate Q_0 for the ruby sample *D*423*L*0.60, it is necessary to analyse the flow regime established for each case in terms of the Reynolds number. According to the boundary layer theory, a low Reynolds number defines a parabolic laminar velocity profile, while flows with high Reynolds numbers have a tendency to present a flat velocity profile, characteristic of a turbulent regime. This difference in the velocity profiles is inherent to the thickness of the boundary layer *d*(x) established inside the microorifice from the inlet edge.

Although the equations available in the literature can not exactly represent the boundary layer development process inside very small devices such as those used in this investigation, they indeed provide the important information that the boundary layer thickness thins with the increase in Reynolds number.

Thus, in the case of an operation under vacuum, the density of the gas is maintained practically constant once the stagnation conditions are stable. Consequently, the Reynolds number is basically dependent on the velocity of the flow that, under a critical flow regime, is maintained constant through an effective flow area, so called critical area. Since the Reynolds number is stable, the boundary layer thickness is constant, what determines a constant critical area providing a steadiness in the volumetric flowrate Q_0.

On the other hand, in the pressurized operation regime, although the stagnation temperature T_0 do not vary that much from the one related to the operation condition under vacuum, the absolute pressure P_0 is much higher, what results in much higher density values for an operation under pressure than for under vacuum. Consequently, the Reynolds numbers also increase with an increase in the pressure P_0, and so, the boundary layer thickness is reduced. Reduction in the boundary layer provides an increase in the critical area available for the flow, even at a critical flow regime making the volumetric flowrate of the gas referred to the stagnation conditions Q_0 to increase as can be seen in the curves presented in the figures 4 to 7.

It is possible to note that, although figures 4 to 7 make it evident that Q_0 is not constant in the critical flow regime for some of the gases used, this increase in the flowrate Q_0 with reduction in the pressure ratio P_b/P_0 is not that emphasized in the case of sample *D*423*L*0.60, as can be seen in the figure 9, since the length *L* available for the development of a boundary layer is relatively short compared to the orifice diameter.

In the case of the ruby samples of smaller diameters, it is possible to verify that this effect is much more pronounced considering that the *L/D* relations are larger in these orifices. Indeed, the effect is markedly higher due to a reduction in the diameter *D*, so that the relation between the boundary layer thickness and the diameter of the orifice *d*(x)/*D* is comparatively larger. This effect can be better visualised, for instance, in the results of Q_0 versus P_b/P_0 presented in figure 10, obtained for the ruby sample *D*034*L*07.4 of diameter *D*=34μm and a relation *L/D*=7,4.

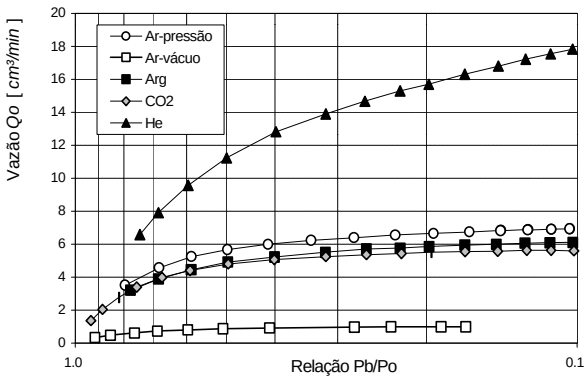

Figure 10. Volumetric flowrate Q_0 versus the pressure ratio P_b/P_0 (sample *D*034*L*07.4, operation under pressure and under vacuum).

Effect of the compressibility factor

Once again, referring to figure 9, it is possible to observe that in the case of an operation with CO_2 gas, the curve of Q_0 shows an opposite tendency to that observed for the other gases used in the investigation, with a relatively pronounced decrease in the flowrate after the critical pressure ratio is attained. This anomalous behaviour of CO_2 gas is directly related to its compressibility factor *Z*.

According to the equation proposed by the API-*American Petroleum Institute* (1981), the compressibility factor Z of a gas can be related to the reduced temperature T_r, to the reduced pressure P_r, and to the accentric factor w which takes into account the unspherical nature of the gas molecules. The proposed relation is given by:

$$Z = 1 + P_r \cdot T_r^{-1} \left[\begin{array}{l} (0{,}1445 + 0{,}073 \cdot \omega) - (0{,}330 - 0{,}46 \cdot \omega) \cdot T_r^{-1} \\ - (0{,}1385 + 0{,}50 \cdot \omega) \cdot T_r^{-2} - (0{,}0121 + 0{,}097 \cdot \omega) \cdot T_r^{-3} \\ - 0{,}0073 \cdot \omega \cdot T_r^{-8} \end{array} \right]$$

where:
P_r : reduced pressure ($P_r = P/P_c$)
P : absolute pressure
P_c : critical pressure
T_r : reduced temperature ($T_r = T/T_c$)
T : absolute temperature
T_c : critical temperature
w : accentric factor

Table 4 below presents the values of P_c, T_c and w for the gases used in the investigation.

Table 4. Critical pressure, critical temperature and accentric factor for the gases used in the investigation.

Gas	Critical pressure P_c [*kPa*]	Critical temperature T_c [*K*]	Accentric factor w
Air	3771	132,45	0,040
Argon	4865	150,8	-0,004
Helium	229	5,3	-0,387
CO_2	7382	304,3	0,231

From: N.V. Nederlandse Gasunie, **Physical Properties of natural gases.** Groningen (1988).

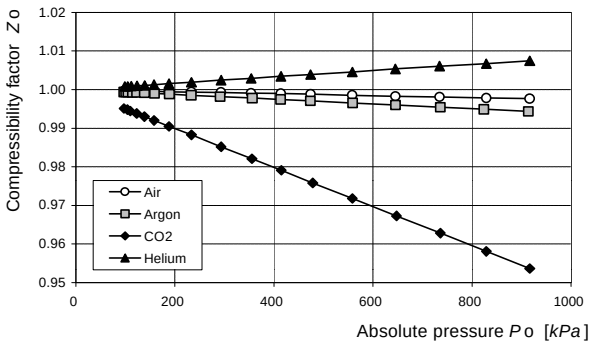

Figure 11. Compressibility factor Z_0 in terms of the absolute stagnation pressure P_0, for T_0=26°C.

Based on these values, and supposing a stagnation temperature T_0=26°C, it is possible to determine the variation of the compressibility factor Z_0 in terms of the absolute stagnation pressure P_0. The values obtained are shown in figure 11.

According to the data presented in figure 11, it is possible to observe that the compressibility factor of the helium gas tends to increase with pressure, while for the other gases Z_0 shows a tendency to decrease with pressure. However, compared to the other gases, the decrease of the compressibility factor for CO_2 is much more evident, and its variation is larger than 4% along the pressure ranges used in the experimental investigation.

Considering that the critical flow regime implies a mass flow proportional to the stagnation pressure, for a perfect gas this represents a constant volumetric flowrate referred to the stagnation conditions, since the density of the gas is directly dependent on this pressure. In the case of an operation under pressure with CO_2 gas, its behaviour is far from a perfect gas, and consequently the effects of compressibility implies that the volumetric flowrate Q_0 necessary to maintain the critical flow regime at the orifice outlet section experiences a small reduction by decreasing the pressure ratio P_b/P_0. This fact explains the shape of the Q_0 curve for the CO_2, shown in the graphic of figure 9.

4.2 Results obtained for the capillaries

The objective of using a set of capillaries was to analyse the behaviour of Fanno flow, characterized by a friction of the fluid with the walls, verifying if the effects caused by the variation of the L/D ratio and maintaining the internal diameter D constant. So, all capillary samples had the same diameter D=427μm, and their lengths L were established between 3,4mm and 68mm. This determined different L/D ratios, in the range of 8 to 160. Roughness at the inner walls of the capillaries was measured and the average value was found to be approximately 1,6μm.

Volumetric flowrate (Q_0) referred to the upstream stagnation conditions

Figures 12 and 13 present the results of volumetric flowrate referred to the stagnation conditions Q_0 in terms of the pressure ratio P_b/P_0, obtained for the set of capillaries operating, respectively, under pressurized and vacuum regimes.

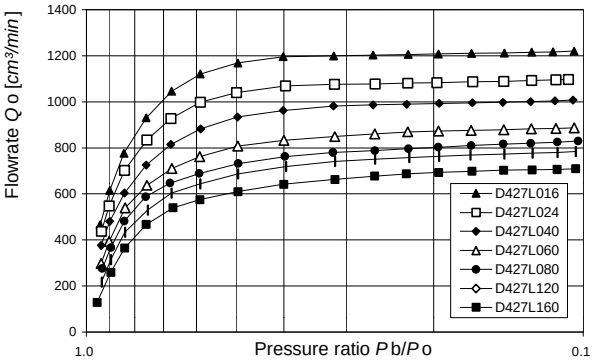

Figure 12. Flowrate Q_0 of air versus the pressure ratio P_b/P_0 (capillary samples, operation under pressure).

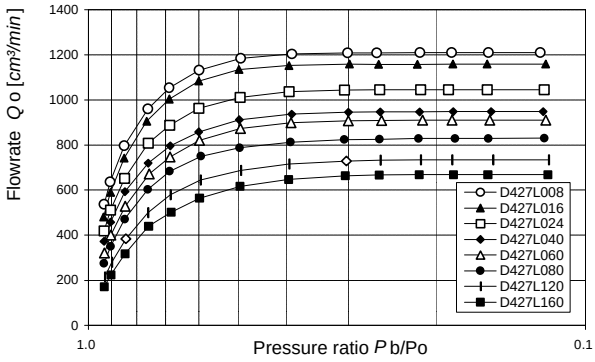

Figure 13. Flowrate Q_0 of air versus pressure ratio P_b/P_0 (capillary samples, operation under vacuum).

Figures 12 and 13 show clearly the differences between the critical flow regimes established under pressure and under vacuum. Similarly to the experimental investigation with the ruby samples, results indicate that the choking condition under a vacuum operation results in a constant volumetric flowrate Q_0 under a critical regime. Under a pressurized regime, however, Q_0 values do not stabilize, presenting a tendency to increase with the reduction in the P_b/P_0 pressure ratio. It is possible to observe also that this effect is more evident for larger *L/D* ratios.

Discharge coefficient

In figures 14 and 15 are presented the experimental values of the discharge coefficients in terms of the Reynolds number referred to the conditions at the inlet section, obtained for the set of 8 capillaries operating, respectively, under pressurized and vacuum regimes.

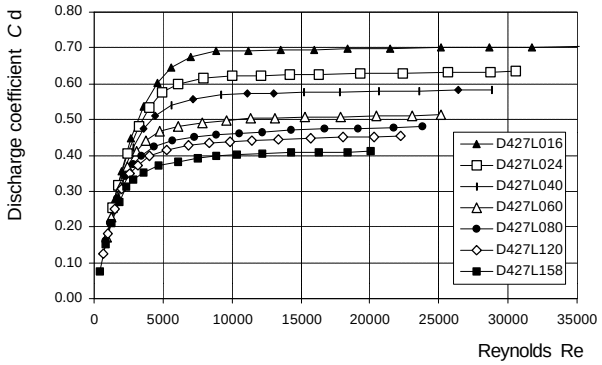

Figure 18. Discharge coefficient C_d versus Reynolds number (capillaries samples, operation with air, operation under pressure).

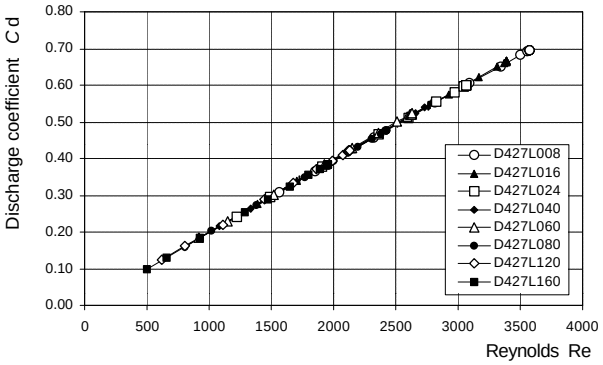

Figure 19. Discharge coefficient C_d versus Reynolds number (capillaries samples, operation with air, operation under vacuum).

Figures 18 and 19 show that the discharge coefficients for a pressurized regime are dependent on the Reynolds number. On the other hand, for an operation under vacuum, once established the critical flow regime, both the discharge coefficient and the Reynolds numbers become constant.

Another fact is that the Reynolds numbers for an operation under pressure are much higher than the respective Reynolds numbers obtained for an operation under vacuum. More, under critical flow regimes, an operation under pressure results in Reynolds numbers characteristic of turbulent flows, while under vacuum, the flow regime theoretically do not necessarily become turbulent for the samples tested.

5. CONCLUSIONS

Experimental results showed that in the range of dimensions of microorifices and capillaries used in the investigation, critical flow regimes is established even at low Reynolds number, the lowest value obtained being of approximately 40. However, it was observed there exists a remarkable difference between the critical flow regimes established under pressurized and vacuum operation conditions.

When the gas flow is generated by a reduction of the pressure in the discharge reservoir, causing a vacuum in the orifice outlet, the flow becomes choked at a certain pressure ratio P_b/P_0. For pressure ratios lower than this critical choking ratio, which presents a different value for each type of sample, the volumetric gas flowrate referred to the stagnation conditions Q_0 remains constant, indicating a stable choking condition and presenting a fixed discharge coefficient. But, for a pressurized regime, where the flow is established by means of an increase of the pressure P_0 in the upstream reservoir, experimental results showed that this choking condition do not remains constant with the reduction of the pressure ratio P_b/P_0.

It was also observed that critical flow regimes are dependent on the type of gas flowing through the orifice, and an important parameter to consider is the compressibility factor of each gas. Among the gases used in the investigation, CO_2 presents an interesting characteristic due to its high compressibility, what determines that the critical flow using this gas presents decreasing flowrate values Q_0 in terms of a reduction of the pressure ratio P_b/P_0, even for an operation under pressure.

Under the point of view of the technological application of the devices used in the investigation, results indicate that orifices and capillaries of small dimensions, operating under a critical flow regime, can be perfectly applied in the measurement and control of low gas flowrates. In the operation under vacuum, the good repeatability of the discharge coefficient of these restriction elements is a real indication that these devices allow flow measurements with relatively low uncertainties, of the order of 1% of the flowrate, depending essentially of the standard used in their calibration.

On the other hand, operating under a pressurized regime, the use of these orifices requires that a previous calibration be performed along the operating pressure ratios P_b/P_0 and, preferably, with the same gas to be used in the operation.

Finally, the present investigation was carried out using orifices and capillaries of small dimensions, and where the miniaturization reveals to be a limiting factor in the manufacturing process, imposing restrictions to the obtainment of samples with controlled geometry and dimensions. However, considering that in most situations the flow was laminar, it was observed that parameters like roundness of the bore and surface roughness did not exert significant influence on the results.

REFERENCES

ANDERSON, J.D.Jr. **Modern compressible flow - With historical perspective.** New York, N.Y., McGraw-Hill Book Company, 1982.

API. **Technical Data Book - Petroleum Refining, metric edition.** Washington, American Petroleum Institute, v.1 and 2, 1981.

N.V. Nederlandse Gasunie, **Physical Properties of natural gases.** Groningen, 1988.

SHAPIRO, A.H. **The dynamics and thermodynamics of compressible flow.** New York, N.Y., John Wiley & Sons, 1953. v.1.

ACKNOWLEDGEMENTS

Authors would like to thank Mr. Paul Baillio from BIRD PRECISION company and PADC/FINEP for the support to this investigation.

Flomeko 2000 - IMEKO TC9 Conference
Salvador, Bahia, BRAZIL
4-8 June, 2000

AUTHORS: Dr. Kazuto Kawakita and Dr. Marcos Tadeu Pereira
IPT-Institute for Technological Research / Flow Laboratory
Cidade Universitária São Paulo / SP
05508-901 BRAZIL
Phone: 55-11-3767-4756
e-mail: kawakita@ipt.br and marcostp@ipt.br